

## Fabrication and compressive performance of plain carbon steel honeycomb sandwich panels

Yu'an Jing<sup>1,2)</sup>, Shiju Guo<sup>1)</sup>, Jingtao Han<sup>1)</sup>, Yufei Zhang<sup>2)</sup>, and Weijuan Li<sup>2)</sup>

1) School of Materials Science and Engineering, University of Science and Technology Beijing, Beijing 100083, China

2) School of Materials Science and Engineering, University of Science and Technology Liaoning, Anshan 114044, China

(Received 2007-06-24)

**Abstract:** Plain carbon steel Q215 honeycomb sandwich panels were manufactured by brazing in a vacuum furnace. Their characteristic parameters, including equivalent density, equivalent elastic modulus, and equivalent compressive strength along out-of-plane ( $z$ -direction) and in-plane ( $x$ - and  $y$ -directions), were derived theoretically and then determined experimentally by an 810 material test system. On the basis of the experimental data, the compressive stress-strain curves were given. The results indicate that the measurements of equivalent Young's modulus and initial compressive strength are in good agreement with calculations, and that the maximum compressive strain near to solid can be up to 0.5-0.6 along out-of-plane, 0.6-0.7 along in-plane. The strength-to-density ratio of plain carbon steel honeycomb panels is near to those of Al alloy hexagonal-honeycomb and 304L stainless steel square-honeycomb, but the compressive peak strength is greater than that of Al alloy hexagonal-honeycomb.

© 2008 University of Science and Technology Beijing. All rights reserved.

**Key words:** steel honeycomb sandwich; brazing; compressive strength; elastic modulus; stress-strain curve

### 1. Introduction

The honeycomb structure is a type of cellular materials with a regular and periodic array of hexagonal cells and is composed of two thin, stiff, strong sheets serving as the primary load carrying elements and a thick layer of low density core providing shear resistance and stiffness [1-2]. It has a wide range of applications, such as aerospace, shipbuilding, vehicle, construction, energy absorbers, thermal isolation components, and packaging materials, because of its excellent structural efficiency, *i.e.*, high strength- and stiffness-weight ratio, elimination of welding, superior insulating quality, and design versatility. A number of reports have focused on the development and research of sandwich structures with honeycomb core [3-6]. From those references, current honeycomb matrix materials mainly included polymer composites, aluminum alloys, titanium, stainless steel, and so on. Many kinds of methods are also available to fabricate sandwich panels because of the difference of demands for mechanical properties and use of matrix material, such as adhesive bond, resistance welding, brazing bond, and transient alloys diffusion [7-10].

In general, the adhesive bond is usually used to manufacture honeycomb because of its low cost, but sometimes, the adhesive bond can not meet the demands for strength. Thus, to increase the bond strength, plain carbon steel honeycomb sandwich panels are brazed using Ag72Cu foils, and their compressive characteristics are investigated in this article. The outline of this article is as follows. First, the procedure used to manufacture plain carbon steel regular hexagonal-honeycombs is described. Second, the elastic parameters are derived, and the compressive behavior is experimentally investigated, including relative density, equivalent elastic modulus, and equivalent compressive strength. Finally, the calculated values are compared with the measurements.

### 2. Manufacturing route

In this study, the regular hexagonal honeycombs were manufactured by brazing in a vacuum furnace, using Q215 plain carbon steel sheets, with a thickness of 0.49 mm. The sheets were cropped into rectangles, widths of 15-25 mm, corresponding to the height of honeycomb panels, and lengths in the range 80-210

mm, corresponding to the width of specimens. The rectangle strips were cold-cripped into corrugated ligaments with cell size  $a=5$  mm by corrugated dies. The corrugated ligaments and the brazing foils were then assembled and clamped tightly to assure stability. The brazing foils were clamped among the corrugated ligaments, the upper and the bottom skinning face. In the vacuum furnace, brazing was carried on with Ag72Cu (wt%) at 830-840 °C for 20 min under  $10^{-3}$ - $10^{-2}$  Pa (as shown in Fig. 1). Capillarity drew the melted braze into the gap at joints, resulting in an excellent bond. The cell size, wall thickness, and relative density of compressive honeycomb specimens manu-

factured in this study are listed in Table 1.

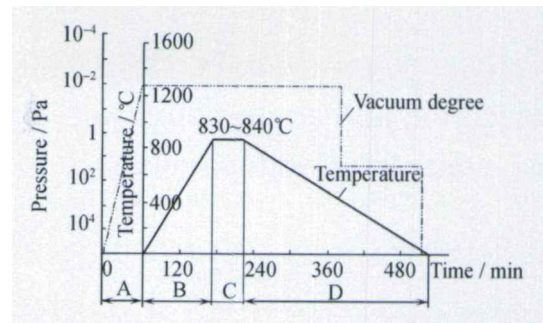


Fig. 1. Temperature and vacuum curves for brazing honeycomb panels: A—pumping time for vacuum; B—heating time; C—holding time for brazing; D—cooling time.

Table 1. Geometry of the regular hexagonal steel honeycomb specimens

No.	Core			Face	Specimens			
	Cell size/ mm	Wall thickness/ mm	Height/ mm	Thickness/ mm	Length/ mm	Width/ mm	Height/ mm	Real density/ ( $\text{kg}\cdot\text{m}^{-3}$ )
T1	5.0	0.49	14.69	0	42.24	38.62	14.69	1030
T2	5.0	0.49	15.00	0.45	39.52	39.00	15.90	1508
T3	5.0	0.49	15.00	0.45	147.49	38.48	15.90	1506
T4	5.0	0.49	15.00	0.45	148.96	44.49	15.73	1503

### 3. Theoretical analysis and mechanical measurements

#### 3.1. Mechanical properties of parent material and brazing joints

The plain carbon steel Q215 was used as the parent material of hexagonal steel honeycombs, including core and skin plates. To measure the change of mechanical properties from parent material, first, the tensile tests were conducted. Tensile specimens of plain carbon steel were cut using electro-discharge machining and subjected to the same brazing cycle used to manufacture the regular hexagonal honeycombs. The measured tensile stress was taken as an elastic linearly hardening stress: Young's modulus  $E=202$  GPa, yield strength  $\sigma_s=213$  MPa before vacuum brazing, Young's modulus  $E=198$  GPa, yield strength  $\sigma_s=165$  MPa after vacuum brazing. The bond strength of brazed joints was measured by tension and shear tests. The tensile strength was 255 MPa, and the shear strength was 144 MPa.

#### 3.2. Theoretical analysis

With the aim to understand the mechanical properties of honeycomb sandwich panels in the preliminary structural design stage, the present study gave firstly the Young's modulus and the strengths of steel honeycomb sandwich panels using simplified mechanic approaches. For simplicity, the detailed procedures were abbreviated, and the schematic view of a honeycomb panel and the size of a cell unit of the honey-

comb core are shown in Figs. 2 and 3, respectively.

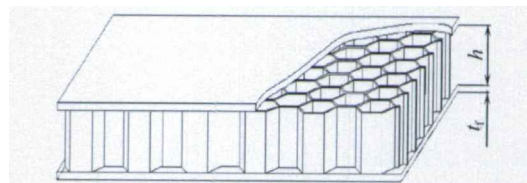


Fig. 2. Schematic view of a honeycomb panel.

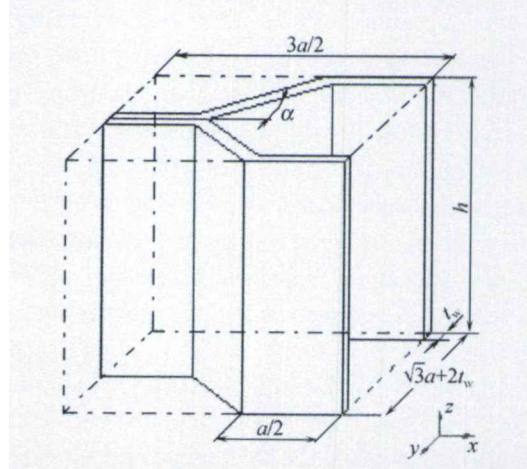


Fig. 3. A cell unit of the honeycomb core and its geometry.

By the equivalent weight method, neglecting the weight of brazing foils, but considering the wall thickness of the honeycomb core, the equivalent density  $\rho_c$  of the hexagonal steel honeycomb core is well described by

$$\rho_c = \frac{8t_w}{3(\sqrt{3}a + 2t_w)} \cdot \rho_0 \quad (1)$$

Similarly, the equivalent density  $\rho$  of the hexagonal

steel honeycomb sandwich panel is given by

$$\rho = \frac{6\sqrt{3}at_f + 12t_ft_w + 8ht_w}{3(\sqrt{3}a + 2t_w) \cdot (h + 2t_w)} \cdot \rho_0 \quad (2)$$

Second, according to the energy equilibrium condition, *i.e.*, the equalization of the work done by external force and the increment of internal energy, the equivalent Young's modulus along thickness (*z*-direction) of the hexagonal honeycomb core can be written as

$$E_{cz} = \frac{8t_w E_0}{3(\sqrt{3}a + 2t_w)} \quad (3)$$

Similarly, the equivalent Young's modulus through the thickness (*z*-direction) of the hexagonal honeycomb sandwich panel is expressed as

$$E_z = \frac{8t_w(h + 2t_f)E_0}{16t_ft_w + 3h(\sqrt{3}a + 2t_w)} \quad (4)$$

According to the theory of bending deformation of a beam, the equivalent Young's moduli through the *x*-direction of the hexagonal honeycomb core and panel can be shown as the following:

$$E_{cx} = \frac{12t_w^3 E_0}{(\sqrt{3}a + 2t_w)(12a^2 + 5t_w^2)} \quad (5)$$

$$E_x = \left[ \frac{2t_f}{h + 2t_f} + \frac{12t_w^3 h}{(\sqrt{3}a + 2t_w)(12a^2 + 5t_w^2)(h + 2t_f)} \right] E_0 \quad (6)$$

The equivalent Young's moduli through the *y*-direction of the hexagonal honeycomb core and panel are given as

$$E_{cy} = \frac{512t_w^3(\sqrt{3}a + 2t_w)E_0}{1152a^2t_w^2 + 2187a^4} \quad (7)$$

$$E_y = \left[ \frac{2t_f}{h + 2t_f} + \frac{512ht_w^3(\sqrt{3}a + 2t_w)}{(h + 2t_f)(1152a^2t_w^2 + 2187a^4)} \right] E_0 \quad (8)$$

Finally, considering the high strength of brazing bond, neglecting the possibility of debonding and delamination, the initial compressive strength is obtained from the force equilibrium conditions as

$$\sigma_{cx} = \frac{2t_f(\sqrt{3}a + 2t_w) + 2t_w h}{(\sqrt{3}a + 2t_w)(h + 2t_f)} \cdot \sigma_s \quad (9)$$

$$\sigma_{cy} = \frac{6at_f + 2t_w h}{3a(h + 2t_f)} \cdot \sigma_s \quad (10)$$

$$\sigma_{cz} = \frac{8t_w}{3(\sqrt{3}a + 2t_w)} \cdot \sigma_s \quad (11)$$

where  $\sigma_s$  is the yield strength of the parent material,

165 MPa. The Eqs.(1)-(11) presented the fundamental characteristic parameters of the hexagonal steel honeycomb core and panel. They are more complex because of the consideration of the effect of the wall thickness of core, but the calculations should be in better agreement with the experimental measurements.

### 3.3. Compression of honeycombs

In this study, to investigate the actual characteristics mentioned above, two experiments, namely the crushing tests under axial compression (*z*-direction) with and without facing skins and the buckling/collapse tests under lateral pressure (*x*- and *y*-directions) with facing skins, were undertaken. The experiments were carried out in a quasi-static manner at a loading speed of 2.0 mm/min using the MTS810 set-up with reference to GB/T1453-87 and ASTM standard D6264-98. The loading system was controlled by a personal computer. The data sets relating the loads were automatically recorded on to the hard disk of the computer in real time, and the displacement and strain of the specimens during compression were recorded by micrometer gauge and strain gauge.

The shapes of the specimen T1 (honeycomb core without facing skins) before and after testing are shown in Fig. 4. From these photographs, the buckling mode can be seen clearly to be torsional-axial and bent buckling of core wall with built-in top and bottom edges. Elastic buckling predominated at low relative pressure, transitioning to plastic buckling at a higher relative pressure. The lateral view photographs of the specimen T2 (honeycomb sandwich panel with facing skins) before and after testing are shown in Fig. 5. Unlike the deformation of the honeycomb core without facing skins, the upper and the bottom facing skins can fix the core wall, so the core wall deformed as plastic bifurcation with three half-wave, and without torsional deformation, only bent buckling of core wall.

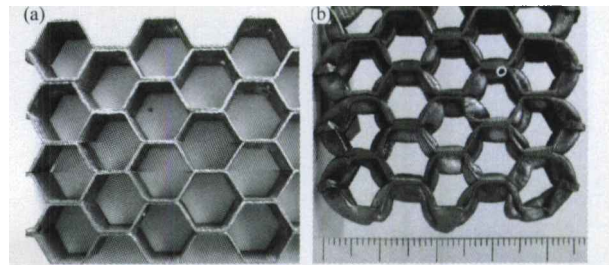


Fig. 4. Top view photographs of specimen T1 before and after testing: (a) undeformed shape before testing; (b) deformed shape after testing.

Also, the shapes of the specimens T3 and T4 before and after testing are shown in Figs. 6 and 7, respectively. From the two photographs, the shape of the

specimen T3 is greater than that of the specimen T4 after compression, that is, the reduction in height of the specimen T3 is less than that of the specimen T4. In practice, the first plastic buckling occurs at the weak spot of the whole honeycomb panel, often on the edge of the two face sheets. And then, the lateral bent of the whole honeycomb appears. Finally, all plastic collapsing occurs regularly on the two face sheets among core walls.

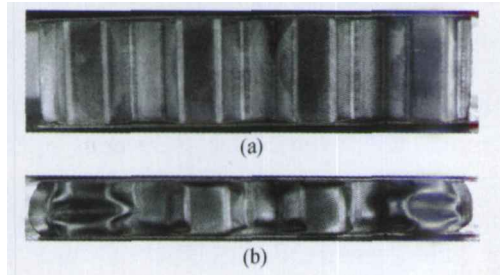


Fig. 5. Lateral view photographs of the specimen T2 before and after testing: (a) undeformed shape before testing; (b) deformed shape after testing.

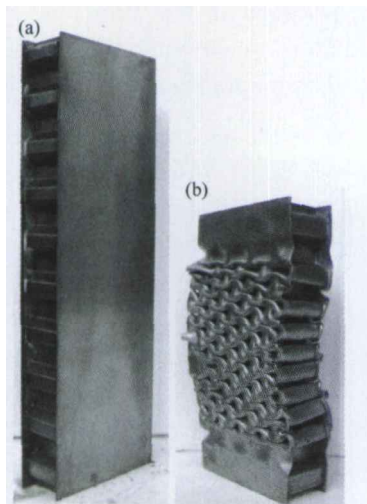


Fig. 6. Shapes of the specimen T3 before and after testing: (a) undeformed shape before testing; (b) deformed shape after testing.

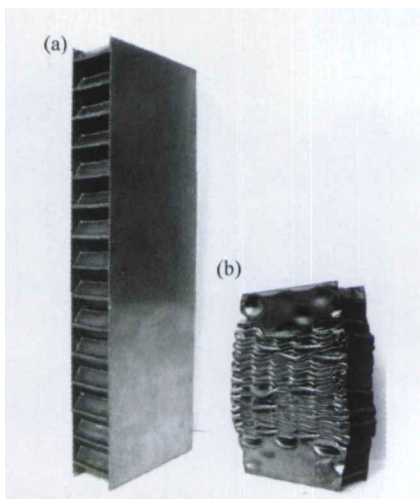


Fig. 7. Shapes of the specimen T4 before and after testing: (a) undeformed shape before testing; (b) deformed shape after testing.

## 4. Results and discussion

### 4.1. Compressive stress-strain curves

The compressive stress-strain curves can be plotted from the data of force and displacement. The force-displacement curves would be greatly different because of the differences of the cross-sections of specimens, so the compressive stress-strain curves are plotted for better comparisons instead of the force-displacement curves. Considering that the errors are little, generally less than 5% original area, the cross-section variations of specimens are neglected while plotting the compressive stress-strain curves. Fig. 8 shows the stress-strain curve of T1 and T2 under axial compression ( $z$ -direction). The measurement of 26.7 GPa equivalent Young's modulus without face-sheets is approximately identical with the measurement of 27.2 GPa equivalent Young's modulus with face-sheets. At the same time, the calculation of equivalent Young's modulus are 27.1 GPa according to Eq. (3), 28.2 GPa according to Eq. (4), with the relative error 1.5% of the former and the relative error 3.5% of the latter.

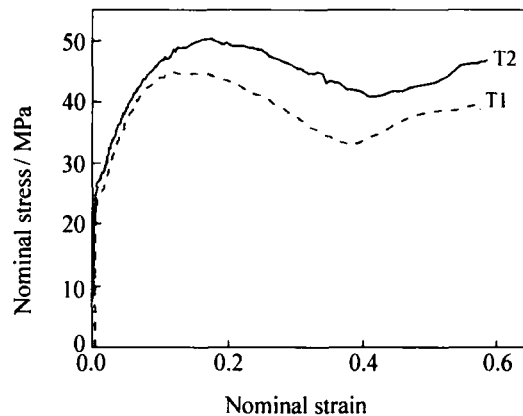


Fig. 8. Compressive stress vs. strain curves ( $z$ -direction) of the specimens T1 (without face-sheets) and T2 (with face-sheets)

Moreover, both the initial compressive strength (elastic buckling strength) and the maximum compressive strength of the specimen T2 are greater than those of the specimen T1. It means that face-sheets fix the core wall and result in the increase of compressive strength. In fact, the measurements of initial compressive strength (elastic buckling strength) and maximum compressive strength (plastic buckling strength) reached 21.6 and 42.6 MPa for the honeycomb core, 24.8 and 49.6 MPa for the honeycomb panel, with the differences of compressive strength of 3-7 MPa, respectively. Also, it should be noted that the compressive nominal stress increased with the nominal strain, but the compressive nominal stress decreased gradually after the peak stress. The minimum compressive

nominal stress was 32 MPa, corresponding to the nominal strain of  $\varepsilon \approx 0.38$  for the honeycomb core, but  $\sigma \approx 41$  MPa corresponding to the nominal strain of  $\varepsilon \approx 0.42$  for the honeycomb panel. After that, the compressive nominal stress increased gradually until the specimens were nearly compressed to solid. The maximum strain was near 0.6 for the specimen T1, near 0.55 for the specimen T2.

Likewise, the stress-strain curves of the specimens T3 and T4 under ( $x$ - and  $y$ -direction) axial compression are also shown in Fig. 9. As shown in Fig. 9, the maximum compressive nominal stress can be up to 22 MPa for the specimen T3 and 15 MPa for the specimen T4, and then the fluctuations occur with the increase of strain. On the one hand, the maximum compressive stress mainly depends on the thickness of two face sheets, not on the thickness of the core wall, but the variation of core wall had greatly influenced on the differences of the maximum compressive stress, e.g., double walls for  $x$ -direction (T3), but single wall for  $y$ -direction (T4). On the other hand, the fluctuations of stress result from the buckles on the two lateral face sheets. It is observed during the tests that the compressive nominal stress decreases as soon as the face sheets among the cell walls begin to buckle, and then increases again. As a matter of fact, there will be many half-wave buckles on the two lateral face sheets. Its number depends on the number of pores in the honeycomb panel (see Fig. 7). For the specimen T3 ( $x$ -direction), the compressive nominal stress starts to rise until the value of strain reaches 0.35, but for the specimen T4 ( $y$ -direction), the compressive nominal stress starts to ascent until the value of strain reaches 0.65 because of the different directions of the compressive axis. Moreover, the equivalent Young's modulus of the specimens T3 and T4 are almost identical to the calculations of 11.3 GPa (see Table 2) according to Eqs. (6) and (8).

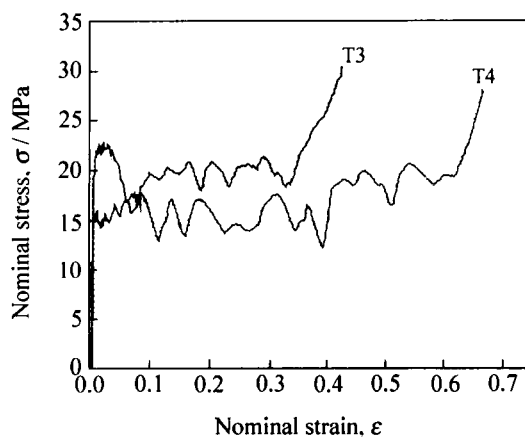


Fig. 9. Compressive stress-strain curves of the specimens T3 and T4

Table 2. Calculations and measurements of equivalent Young's modulus of steel honeycomb specimens

No.	Equivalent Young's modulus, $E$ / GPa	
	Calculation	Measurement
T1	27.1	26.7
T2	28.2	27.2
T3	11.3	11.1
T4	11.3	10.8

#### 4.2. Comparison of theoretical analysis with measurements

A comparison of the calculations according to Eqs. (3)- (8) with the measurements of equivalent Young's modulus is shown in Fig. 10 by plotting the equivalent Young's modulus against the ratio of wall thickness to cell size with the elastic Poisson's ratio taken to be 0.3.

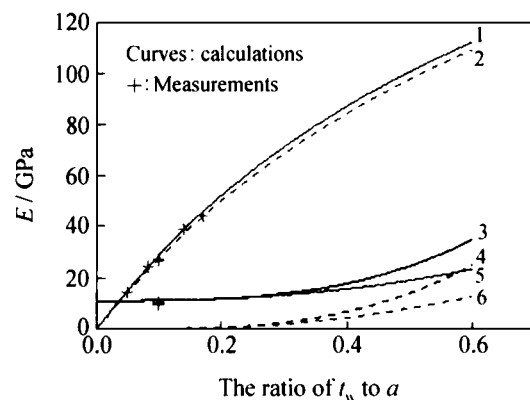


Fig. 10. Comparison of the calculations with measurements of equivalent Young's modulus: 1—honeycomb sandwich panel ( $z$ -direction); 2—honeycomb core alone ( $z$ -direction); 3—honeycomb sandwich panel ( $x$ -direction); 4—honeycomb core alone ( $x$ -direction); 5—honeycomb sandwich panel ( $y$ -direction); 6—honeycomb core alone ( $y$ -direction)

The following findings can be obtained from Fig. 10. First, all measurements of equivalent Young's modulus are in good agreement with the calculations, also listed in Table 2. Second, the equivalent Young's modulus of  $z$ -direction strongly increases with the ratio of  $t_w$  to  $a$  and is far greater than those of  $x$ - and  $y$ -directions. In contrast, the equivalent Young's moduli of  $x$ - and  $y$ -directions slowly increase with the ratio of  $t_w$  to  $a$ . The initial values of equivalent Young's moduli of  $x$ - and  $y$ -directions with face-sheets vary with the thickness of face-sheets (see the curves 3 and 5 in Fig. 10) and are strongly affected by bonding face-sheets. As a matter of fact, both the initial values of equivalent Young's modulus and compressive strength of  $x$ - and  $y$ -directions mainly depend on the thickness and the mechanical properties of two face-sheets. In addition, the equivalent Young's moduli of  $x$ - and  $y$ -directions of the honeycomb core

alone can be neglected and taken as soft-core while the ratio of  $t_w$  to  $a$  is less than 0.2. Thus, the equivalent Young's modulus of  $x$ -direction is nearly equal to that of  $y$ -direction when the ratio of  $t_w$  to  $a$  is less than 0.35.

### 4.3. Comparison of plain steel honeycombs with aluminum honeycombs

In this study, measurements of the out-of-plane compressive response of a commercial Al alloy hexagonal honeycomb [1] and the 304L stainless steel square-honeycomb [11] are obtained and contrasted with those of the steel honeycomb panels. The Al alloy hexagonal-honeycomb is made from a 3003-grade aluminum alloy (yield strength  $\sigma_y \approx 210$  MPa) manufactured using cold expansion, with the relative density  $\rho_e = 0.03$ , and a maximum strength of 2.3 MPa. Fig. 11 shows the comparison of the dependence of the ratio of normal stress to equivalent density on the nominal strain  $\epsilon$  among Al alloy hexagonal honeycomb, 304L stainless steel square-honeycomb, and plain carbon steel hexagonal honeycomb.

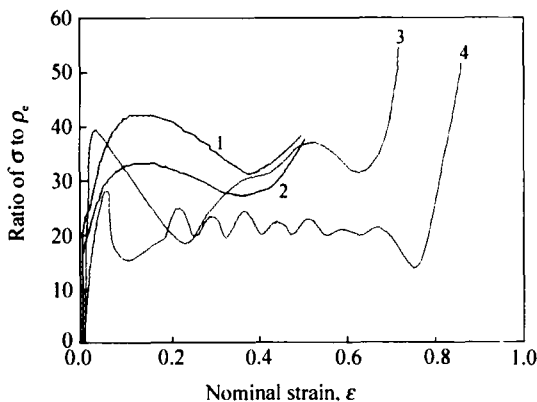


Fig. 11. Comparison of the dependence of the ratio of  $\sigma$  to  $\rho_e$  on the nominal strain  $\epsilon$ : 1—honeycomb core alone ( $z$ -direction); 2—honeycomb sandwich panel ( $z$ -direction); 3—304L stainless steel square-honeycomb; 4—Al alloy hexagonal-honeycomb.

As shown in Fig. 11, the ratio of  $\sigma$  to  $\rho_e$  of plain carbon steel hexagonal honeycomb is nearly equal to that of 304L stainless steel square-honeycomb, and both are slightly higher than that of Al alloy hexagonal-honeycomb. So it can be inferred that the ratio of  $\sigma$  to  $\rho_e$  is likely to be greater than that of Al alloy while being prepared by high strength steel. Moreover, unlike the post-buckling response of Al alloy hexagonal-honeycomb, the post-buckling response of plain carbon steel hexagonal honeycomb varied gently. This difference in post-buckling response might be attributed to the differing strain-hardening capacity of the cell wall material. That is, the high strain hardening of the steel surpassed that of Al alloy, so the formation of successive folds is slow.

## 5. Summary and conclusions

The manufacturing route of honeycomb using plain carbon steel was developed for the first time. And then, the study focused on deducing theoretical equations that permit the computation of equivalent Young's modulus as well as initial strength considering the thickness of core wall for hexagonal honeycomb sandwich, subjected to out-of-plane and in-plane forces. The measured stress-strain curves show that the measurements of equivalent Young's modulus and initial compressive strength are in good agreement with calculations, and that the maximum compressive strain near to solid can be up to 0.5-0.6 along out-of-plane and 0.6-0.7 along in-plane. The ratio of  $\sigma$  to  $\rho_e$  of plain carbon steel regular hexagonal honeycomb is near to those of Al alloy hexagonal-honeycomb and 304L stainless steel square-honeycomb, but the compressive peak strength is greater than that of Al alloy hexagonal-honeycomb.

## References

- [1] L.J. Gibson and M.F. Ashby, *Cellular Solids: Structure and Properties*, 2nd ed, Cambridge University Press, Cambridge, 1997, p.12.
- [2] Y.J. Chen, X.Q. Zuo, and Q.N. Shi, Development and application of honeycombed metal, *Mater. Rev.* (in Chinese), 17(2003), No.12, p.32.
- [3] J.K. Paik, A.K. Thayamballi, and G.S. Kim, The strength characteristics of aluminum honeycomb sandwich panels, *Thin Walled Struct.*, 35(1999), p.205.
- [4] H.X. Zhu and N.J. Mills, The in-plane non-linear compression of regular honeycombs, *Int. J. Solids Struct.*, 37(2000), p.1931.
- [5] D. Karagiozova and T.X. Yu, Plastic deformation modes of regular hexagonal honeycombs under in-plane biaxial compression, *Int. J. Mech. Sci.*, 46(2004), p.1489.
- [6] M.H. Fu and J.R. Yin, Equivalent elastic parameters of the honeycomb core, *Acta Mech. Sin.* (in Chinese), 31(1999), No.1, p.113.
- [7] H.N.G. Wadley, N.A. Fleck, and A. G. Evans, Fabrication and structural performance of periodic cellular metal sandwich structures, *Compos. Sci. Technol.*, 63(2003), p.2331.
- [8] R.J. Feng and J.M. Yu, Honeycomb filled board and its application in automotive industry, *Automob. Technol. Mater.* (in Chinese), 2003, No.8, p.30.
- [9] J. Zhang, F. Feng, and Y.M. Zhu, A study on bonding process of aluminum honeycomb sandwich panel. *Electro Mech. Eng.* (in Chinese), 21(2005), No.2, p.41.
- [10] W.S. Burton and A.K. Noor, Structural analysis of the adhesive bond in a honeycomb core sandwich panel, *Finite Elem. Anal. Des.*, 1997, No.26, p.213.
- [11] F. Côté, V.S. Deshpande, and N.A. Fleck, The out-of-plane compressive behavior of metallic honeycombs, *Mater. Sci. Eng. A*, 380(2004), p.272.